Spatial and temporal progression of internal erosion in cohesionless soil

Ricardo Moffat, R. Jonathan Fannin, and Stephen J. Garner

Abstract: Permeameter tests were performed on four widely graded cohesionless soils, to study their susceptibility to internal erosion. Test specimens were reconstituted as a saturated slurry, consolidated, and then subjected to multi-stage seepage flow under increasing hydraulic gradient. The occurrence of internal instability is described qualitatively, from visual observations through the wall of the permeameter during a test and from post-test observations; it is also described quantitatively, from change of hydraulic gradient within the specimen and from axial displacement during a test. The results provide a novel insight into the spatial and temporal progression of seepage-induced internal instability. This insight yields an improved characterization of suffusion and suffosion in cohesionless soils, the progression of which appears governed by a critical combination of hydraulic gradient and effective stress.

Key words: internal instability, suffusion, suffosion, piping.

Résumé : Des essais en perméamètre ont été réalisés sur quatre sols sans cohésion et à granulométrie étalée afin d'étudier leur susceptibilité à l'érosion interne. Les échantillons ont été reconstitués sous forme de pulpe saturée, consolidée et ensuite soumise à un écoulement multi-étapes sous un gradient hydraulique qui augmente. L'apparition de l'instabilité interne est décrite de façon qualitative, à partir d'observations visuelles à travers la paroi du perméamètre durant l'essai, ainsi que par des observations post-essai. L'instabilité interne est aussi décrite quantitativement à partir des variations du gradient hydraulique à l'intérieur des échantillons et du déplacement axial durant l'essai. Les résultats offrent une vision nouvelle de la progression spatiale et temporelle de l'instabilité interne causée par l'infiltration. Ces résultats apportent une meilleure caractérisation de la suffusion et de la suffosion dans les sols sans cohésion; leur progression semblant être gérés par une combinaison critique du gradient hydraulique et de la contrainte effective.

Mots-clés : instabilité interne, suffusion, suffosion, renard.

[Traduit par la Rédaction]

Introduction

In widely graded cohesionless soils, such as those used in construction of many earth dams, the term "internal instability" refers to the inability of the coarser fraction of a soil to prevent migration of its finer fraction as a result of seepage flow (Fell et al. 2005). The action differs from that of contact or surface erosion (Reddi et al. 2000). The phenomenon of internal instability takes different forms and is described by several terms. Kovacs (1981, p. 350) described internal suffusion as the "redistribution of fine grains within the layer … when the solid volume of the layer is not changed, only the local permeability is altered." Bendahmane et al. (2008) found a gain in the rate of suffusion with increased hydraulic gradient and with reduced confining stress, from triaxial tests on sand with different clay content. Kenney and Lau (1985, p. 215) similarly used suffosion to describe "the transport of small particles from a soil." Yet in general usage, suffusion describes the action of "overspreading, as with a liquid; to fill or cover, as with something fluid," and is considered distinct from suffossion, which describes the action of "digging under or up; undermining" (OED online 2010). In the geological context of landform processes, suffosion has been used to describe "bursting out on the surface, in little eruptions, of highly mobile or water-saturated material" (Bates and Jackson 1987, p. 660). Furthermore, Chapuis (1992, p. 711) described suffosion as "the transport of small particles from a soil, which leaves large openings between the particles."

Accordingly, and recognizing the need for clarity of terms when reporting on seepage-induced internal instability, a distinction can be reasonably made between suffusion, where the finer fraction of an internally unstable soil moves within the coarser fraction without any loss of matrix integrity or change in total volume, and suffosion, where particle migration yields a reduction in total volume and a consequent potential for collapse of the soil matrix (Richards and Reddy 2007). The retrogressive phenomenon of piping in embankment dams describes "the progressive development of internal erosion by seepage, appearing downstream as a hole … discharging water" (ICOLD 1978, p. 44). This qualitative distinction between the phenomena of suffusion, suffosion, and piping is used herein to describe the spatial and

Received 21 September 2009. Accepted 9 August 2010. Published on the NRC Research Press Web site at cgj.nrc.ca on 1 March 2011.

R. Moffat. Department of Civil Engineering, University of Chile, Blanco Encalada 2002, Santiago, Chile.
R.J. Fannin.[1] Department of Civil Engineering, The University of British Columbia, 6250 Applied Science Lane, Vancouver, BC V6T 1Z4, Canada.
S.J. Garner. BC Hydro and Power Authority, 6911 Southpoint Drive, Burnaby, BC V3N 4X8, Canada.

[1]Corresponding author (e-mail: jonathan.fannin@ubc.ca).

temporal progression of internal instability in laboratory permeameter tests.

Empirical methods have been proposed to evaluate the potential for internal instability. They are based on the shape of the gradation curve and, more specifically, the variation in grain size over a designated portion of the curve. Kezdi (1979, p. 125) reported the structure of a widely graded soil "is such that the pores of one fraction will be just filled by the grains of the next fraction … If water moves through the soil, then the soil can be taken to be composed of two components, one of them serving as a filter for the grains of the other." For reporting purposes herein, grains with potential to move through the pore structure of a soil are described as the finer fraction. Kezdi (1979) further proposed an index ratio of D'_{15}/d'_{85}, based on splitting the gradation to yield D'_{15} of the coarse fraction and d'_{85} of the finer fraction. An index ratio $D'_{15}/d'_{85} = 4$ was advocated for stability, and derived independently by de Mello (1975) and Sherard (1979); the methodology was subsequently recognized by ICOLD (1986). Fannin and Moffat (2006) demonstrated experimentally that gradations close to that limit value appear stable, whereas a soil with $D'_{15}/d'_{85} \approx 7$ exhibited instability at relatively low gradient. In a similar approach, Kenney and Lau (1985) proposed an alternative index ratio, H/F, for a methodology that is recognized by the Canadian Dam Association (CDA 2007). The gradation curve is split to establish the incremental mass fraction passing (H) over a range of grain diameter D to $4D$, which is compared with the mass passing (F) at the lower limit of the interval D. A threshold value of $H/F = 1$ was advocated at $F < 0.2$ in soil having a widely graded coarse fraction and at $F < 0.3$ in soil with a narrowly graded coarse fraction (Kenney and Lau 1986), based on interpretation of laboratory data and taking into account experience from engineering practice (Milligan 1986). The general applicability of each index ratio for internal stability was confirmed from laboratory permeameter tests (Skempton and Brogan 1994). Laboratory observations of self-filtration led Raut (2006) to postulate that the method is likely conservative, a finding also confirmed by Wan and Fell (2008). Li and Fannin (2008) demonstrated, from a database of 57 gradations compiled from eight published laboratory studies, that the Kezdi (1979) method is relatively more conservative for $F < 0.15$ and the Kenney and Lau (1985) method is more conservative for $F > 0.15$.

It is important to recognize that unstable gradations are deemed to have potential for instability, with the onset controlled by the nature of the flow regime in the soil and triggered where seepage-induced forces exceed a critical threshold. Kenney and Lau (1985, p. 218) acknowledged "conditions used in the tests to cause particle transport were severe," and did not attempt to control the combination of hydraulic gradient and mild vibration imposed on the test specimens. Indeed, little is known about the hydromechanical constraints to instability, or the development of that instability, leading Skempton and Brogan (1994, p. 459) to observe that "further work is required to define more closely the relation of critical gradient and stability index" in a soil.

The W.A.C. Bennett Dam is located on the Peace River, in the Province of British Columbia. It is a zoned earthfill embankment, 183 m high and 2 km long, that was constructed between 1964 and 1968. The core of the dam is a widely graded nonplastic silty sand with some gravel, which was processed from a moraine deposit that was found deficient of particles in the 2.0 to 4.76 mm range; a small amount of nonplastic sandy silt was blended with the moraine during processing (Morgan and Harris 1967). Downstream of the core are two filter zones, also processed from the moraine, the first of which is termed a transition zone. Details on the configuration of the zoned embankment dam, and specified gradation envelopes for the soil of each zone, are given by Ripley (1967). Gradation limits of the various zones in the dam were selected to accommodate a reasonable variation in the moraine deposit: a summary of gradation curves found in the construction records is reported by Li et al. (2009). The dam operated without incident until 1996, when the discovery of two sinkholes (Stewart and Watts 2000) led to a program of field monitoring and laboratory research to better understand the nature of internal instability within the embankment (Garner and Fannin 2010). The objective of this paper is to report the spatial and temporal progression of internal instability in four cohesionless soils, from multi-stage seepage tests in a large permeameter. The test specimens were reconstituted from samples of core and transition material taken at the W.A.C. Bennett Dam. Visual observation and experimental measurement have provided a comprehensive description of instability, enabling the phenomena of suffusion, suffosion, and piping to be properly distinguished. The observations, together with measurements of water head distribution along the length of the test specimen, yield new insights into the movement of finer fraction particles, onset of instability, and nature of instability development within the soil specimen.

Soil specimens

Four soils were provided by BC Hydro and Power Authority and used in testing; they are believed representative of earthfill materials present in select zones of the W.A.C. Bennett Dam. Two soils are widely graded gravel and sand (see Fig. 1), one of which has no fine particles less than 0.075 mm (T-0) and the other a fines content of 5% (T-5). Two soils are widely graded gravel, sand, and silt, for which the fines content is 20% (C-20) and 30% (C-30). All four soils exhibit a subtle gap in the gradation curve, which is found to be more pronounced in the T-0 and T-5 soils.

The T-0 and T-5 soils have a grain size range that is comparable to the sand and gravel specimens tested by Kenney and Lau (1985) in development of the empirical H/F stability index. Evaluation of the gradation curves for T-0 and T-5 yields an $(H/F)_{min}$ of 0.95 and 0.9, respectively, at a value of $F = 0.2$ (Fig. 2*a*). Strictly speaking, they fail to satisfy the internal stability criterion of $H/F \geq 1$ at $F \leq 0.2$, and therefore are deemed susceptible to internal instability. From inspection, the H/F ratio diminishes to a very small value at $F = 0.38$ where a gap occurs in the gradation curve. The C-20 and C-30 soils are considerably finer than those tested by Kenney and Lau (1985), and therefore the extent to which the empirical H/F criterion for internal instability may be applied to these silty soils is uncertain. Nevertheless, analysis yields $(H/F)_{min} = 0.67$ for both soils at $F = 0.2$ (Fig. 2*a*).

A companion evaluation was made using the Kezdi (1979) stability index (see Fig. 2*b*). In the absence of a sug-

Fig. 1. Grain-size distribution curves.

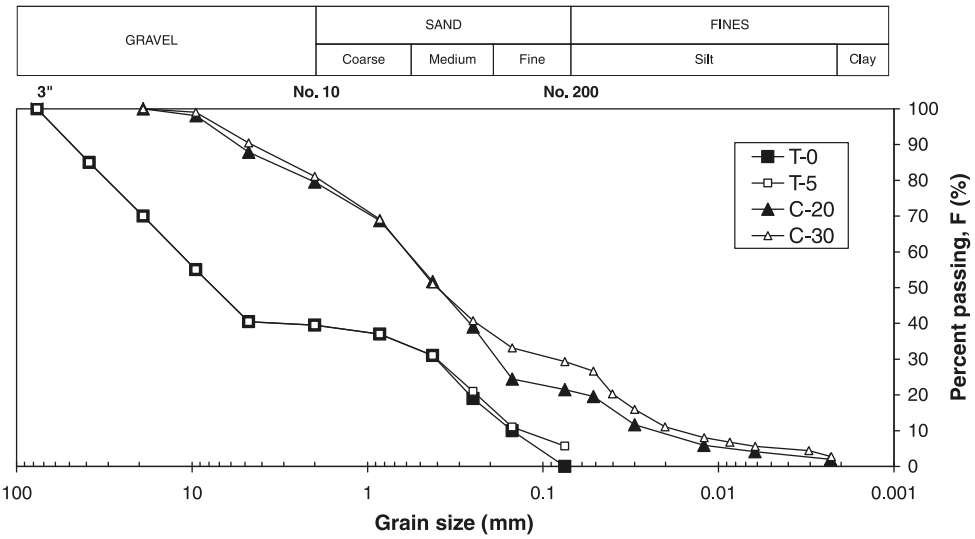

Fig. 2. Evaluation of internal stability: (*a*) Kenney and Lau (1986) method; (*b*) Kezdi (1979) method.

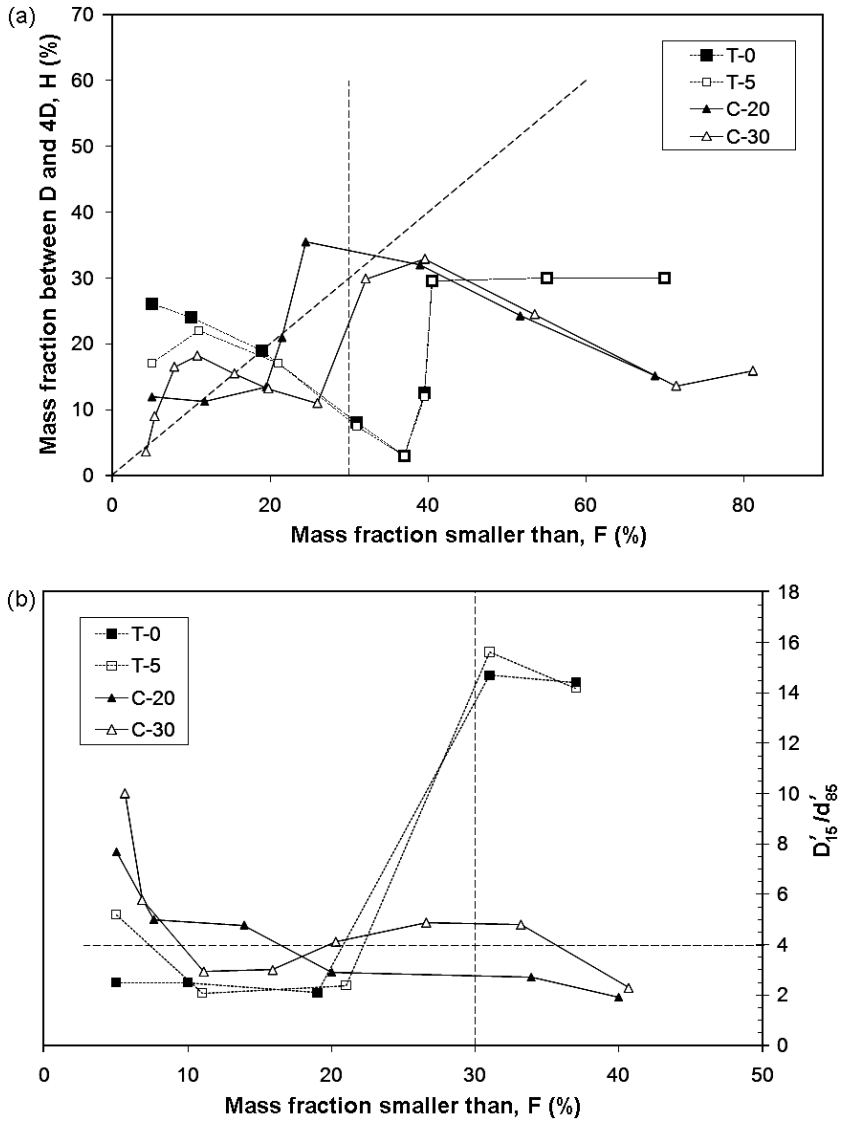

gested limit value of F for purposes of gradation analysis, the index ratio $(D'_{15}/d'_{85})_{max}$ is evaluated to a nominal limit of $F \leq 0.3$, recognizing that coarser particles are supported in a matrix of finer particles when F exceeds approximately 0.35 (Skempton and Brogan 1994). All four gradations fail to satisfy a threshold value of $(D'_{15}/d'_{85})_{max} \leq 4$, most notably the T-0 and T-5 soils, both of which exhibit a maximum value of nearly 15 (Fig. 2*b*).

These geometric analyses of particle-size distribution curves, made with reference to empirical criteria, suggest all four soils are susceptible to internal instability. More specifically, comparison implies the sandy gravels (T-5 and T-0) are likely more susceptible than the silt, sand, and gravel mix (C-30 and C-20), based on the relative magnitude of $(D'_{15}/d'_{85})_{max}$ values within $F \leq 0.3$ and based on $(H/F)_{min}$ values within $F \leq 0.3$. Yet the two methods evaluate a potential for instability according to a geometric constraint, namely the ability of the coarser fraction to prevent migration of the finer fraction. They do not provide any insight into the nature of that internal erosion or the critical gradient to trigger its onset.

Laboratory permeameter

A laboratory permeameter was designed and commissioned to enable reconstitution of a soil specimen that, upon completion of a stage of consolidation, is subjected to unidirectional seepage flow. The design was based on earlier experience reported by Garner and Sobkowicz (2002). The permeameter comprises a cylindrical cell that mounts in a reaction frame, a system to apply axial loading to the soil speceimen, and a system to maintain one-dimensional seepage flow through the soil. A detailed description of the permeameter has been given by Moffat and Fannin (2006), from which a brief summary is provided herein.

The rigid-wall permeameter is made of a transparent acrylic tube to allow visual observation of the specimen during testing. It accommodates a specimen of diameter 279 mm, which was reconstituted and consolidated to an initial length (L_c) in the range 325 to 550 mm. The specimen is supported on a lower wire mesh screen of 2.76 mm (soil types T-0 and T-5) or 0.15 mm opening size (soil types C-20 and C-30). Axial load is applied using a porous loading plate, which seats against an upper wire mesh screen on the top surface of the specimen. Opening sizes of the wire mesh at the exit boundary of the specimen are reported in Table 1. The load imparts a constant vertical effective stress to the top of the specimen that is maintained by a feedback control system (Moffat and Fannin 2006).

An array of transducers was used to monitor the spatial and temporal progression of any internal erosion, thereby characterizing the phenomena of suffusion, suffosion, and piping (Fig. 3). Vertical effective stress on the top of the specimen was deduced from the axial force, measured with a load cell. Displacement of the top plate (δ) was measured using a linear variable differential transformer (LVDT) and used to record change in initial specimen length. Volumetric flow rate through the soil was determined from change in the mass of water held in an inflow and outflow tank to the permeameter. Pore-water pressure was measured at seven locations on the permeameter wall with an array of total pressure transducers (TPT 1 to TPT 7), and a companion array of differential pressure transducers (DPT 1 to DPT 6), from which the variation of local hydraulic gradient (i_{jk}) between any two port locations along the length of the specimen was established as shown in Fig. 3 (see the inserted diagram).

Table 1. Select test details.

Test code	Length, L_c (mm)	Exit wire mesh (mm)	Duration of seepage flow
T-0-25-D	552	2.76	13 h 47 min
T-5-175-U	440	2.76	32 h 5 min
C-20-50-U	340	1.14	112 h 22 min
C-30-80-U	335	1.14	192 h 55 min

Test procedure

Variables examined in permeameter testing were soil type (T-5, T-0, C-30, and C-20), vertical effective stress on the top surface of the soil specimen (25 to 175 kPa), average hydraulic gradient (1 to 45), and direction of seepage flow in the permeameter (upward or downward). The test code, for example T-0-25-D, defines the combination of soil type (T-0), effective stress (25 kPa), and flow direction (downward).

Test specimens were reconstituted using the method of batched slurry mixing of the soil in a vacuum chamber, followed by discrete deposition in the permeameter under a thin film of standing water (Moffat and Fannin 2006). This method yields a very loose, saturated soil specimen. Subsequent application of axial load to achieve a desired value of vertical effective stress imposed a stage of consolidation settlement, which occurred relatively quickly in T-0 and T-5 soils and more slowly in C-20 and C-30 soils.

Unidirectional flow of filtered de-aired water was imposed in either an upward or downward direction, by means of a feedback system to maintain a constant average hydraulic gradient, i_{av}, across the specimen length. A multistage test procedure was used. All tests began with a stage at $i_{av} \approx 1.0$. Thereafter, seepage flow was increased by increments of $\Delta i_{av} \approx 1.0$ until internal instability occurred or the capacity of the test device was exceeded. The duration of each stage was typically 90 min. However, for C-20 and C-30 soils, the duration was occasionally increased to as much as 24 h to obtain sufficient volumetric discharge to calculate a value of hydraulic conductivity. Following the onset of any internal instability, seepage flow was typically stopped to allow visual observation of the condition of the specimen during removal from the permeameter.

Select test results

The nature of internal instability observed in testing is described primarily from interpretation of axial displacement and hydraulic gradient, and verified by visual observations through the wall of the permeameter. The response of each soil is described herein with reference to a single combination of test variables, thereby providing a detailed illustration of the spatial and temporal progression of instability phenomena.

Fig. 3. Specimen deformation with increased seepage.

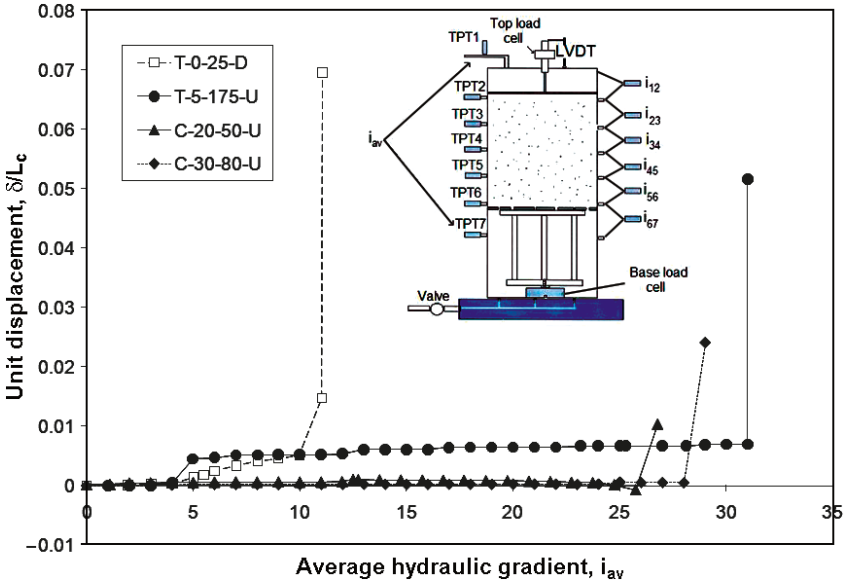

"Clean" gravel and sand (test T-0-25-D)

The T-0 soil was consolidated under a top vertical effective stress of 25 kPa to an initial length of 552 mm and then subjected to downward flow. Seepage flow was initiated at i_{av} = 1.0 and increased by increments of approximately 1 to a value i_{av} = 11 over a cumulative time of nearly 14 h of seepage flow (Table 1). The variation of unit displacement (δ/L_c) with increasing i_{av} shows negligible vertical movement to $i_{av} \leq 4$ (Fig. 3). Small movements occurred at $5 \leq i_{av} \leq 10$, prior to the development of a relatively large displacement during the final stage at i_{av} = 11. This latter deformation is attributed to the onset of significant erosion within the specimen.

The variation of local hydraulic gradient i_{jk} with time during the final stage of the test is shown in Fig. 4 (see insert of Fig. 3 for port locations). The value of i_{av} = 11 was applied slowly over a period of nearly 200 s. Differences in the resulting values of i_{jk} are attributed to spatial variations in hydraulic conductivity arising from earlier stages of the test. The i_{jk} values are essentially constant with time in this final stage, which confirms a period of relative stability to an elapsed time of approximately t = 750 s. Thereafter, a significant change took place. Specifically, i_{56} exhibited a sudden decrease, followed almost immediately by a similar decrease in i_{45}. The behavior implies a local increase in hydraulic conductivity, which is attributed to the onset of instability. A companion increase occurred in i_{23} and i_{34} as a direct consequence of the control system seeking to maintain the target i_{av} = 11 across the specimen length. In the lowermost zone, i_{67} exhibited no significant change with time. In the uppermost zone, i_{12} dropped from a value of 14 to almost 0 in about 100 s, as axial compression of the specimen caused the top plate to pass below the location of port 2 on the permeameter wall.

Visual observations have been found very useful to the interpretation of these test data. Every increment of downward hydraulic gradient to i_{av} = 10 caused a washout of relatively fine particles at the lower wire mesh boundary, yielding a discoloration of the outflow water (for example, see Fig. 5*a*, at i_{av} = 5). Yet, no companion particle movement was evident at the contact of the specimen with the inside wall of the permeameter. Visual inspection of particle loss through the lower wire mesh revealed that particle loss was not uniform across the exit boundary. Rather it occurred at preferential locations, and those locations were observed to change with each new increment of gradient. The particle loss diminished with elapsed time during each stage, causing the discharge flow to become clear with time (for example, see Fig. 5*b*, at i_{av} = 10). In contrast to earlier test stages, raising i_{av} to 11 generated a relatively significant loss of soil. At the onset of instability ($t \approx 750$ s, see Fig. 4), particle movements were observed between the middle of the specimen (near port 4, see inserted diagram of Fig. 3) and its downstream outlet at the base. The movements led to development of a short preferential flow channel at $t \approx 1180$ s that became choked by a process of episodic particle rearrangement and infilling over a period of 60 s (compare Figs. 6*a* and 6*b*). Another short channel was observed higher on the specimen at $t \approx 1360$ s, suggesting a retrogressive advance in the upstream direction (Fig. 6*c*). At t = 2380 s, a large vertical to subvertical channel was observed in the specimen above its downstream outlet, oriented in the direction of the short channel noted previously. Soon thereafter, a continuous pipe developed across the entire length of the specimen, whereupon the test was stopped.

A forensic examination was conducted on all specimens after testing by means of exhuming each specimen as a series of thin layers to establish the spatial extent of any piping activity. Although the affected cross-sectional area was large in test T-0-25-D (see Fig. 7), visual observations indicate that it occurred mainly within the body of the test specimen and involved only a relatively small contact area at the permeameter wall.

Gravel and sand, with trace of silt (test T-5-175-U)

The T-5 soil was consolidated under a vertical effective stress of 175 kPa, to an initial length of 440 mm, and then

Fig. 4. Onset of instability: test T-0-25-D (i_{av} = 11).

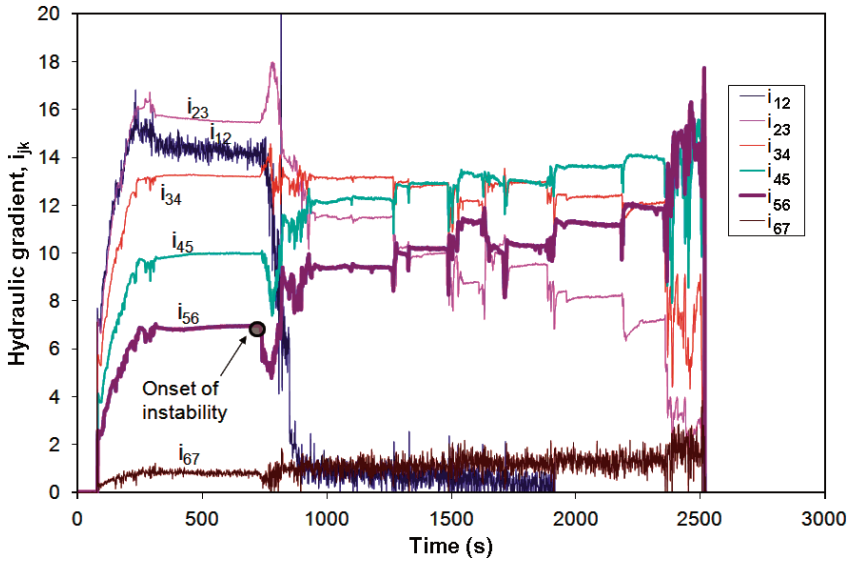

Fig. 5. Visual observation of suffusion, test T-0-25-D; (*a*) i_{av} = 5; (*b*) i_{av} = 10.

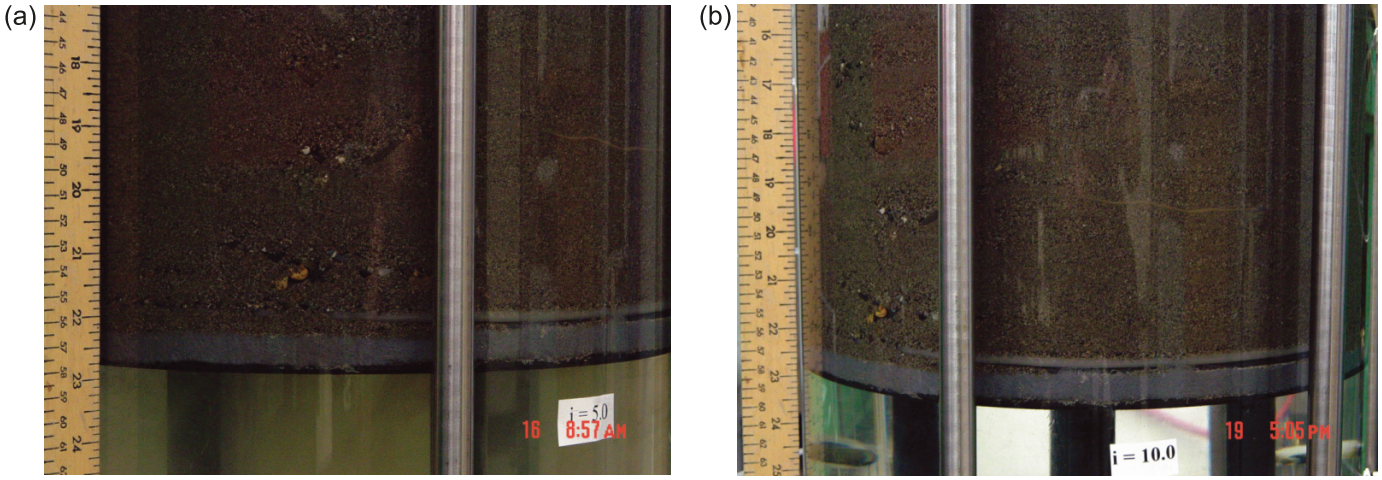

Fig. 6. Visual observation of suffosion, test T-0-25-D (i_{av} = 11): (*a*) *t* = 1180 s; (*b*) *t* = 1240 s; (*c*) *t* = 1360 s.

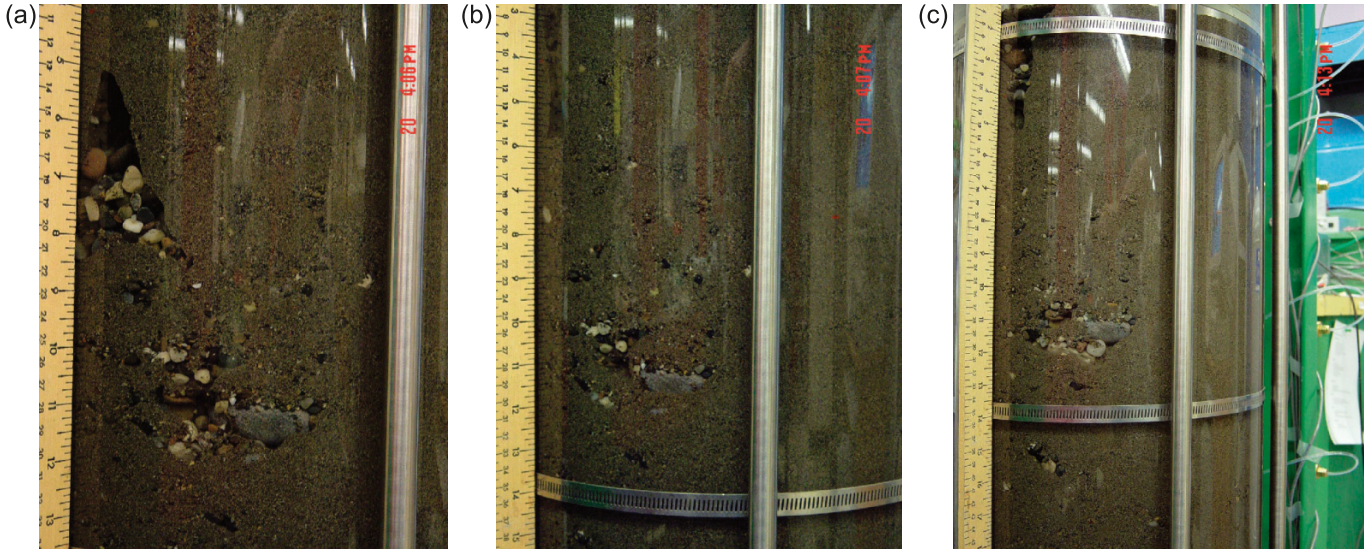

Fig. 7. Spatial extent of soil "pipe": test T-0-25-D.

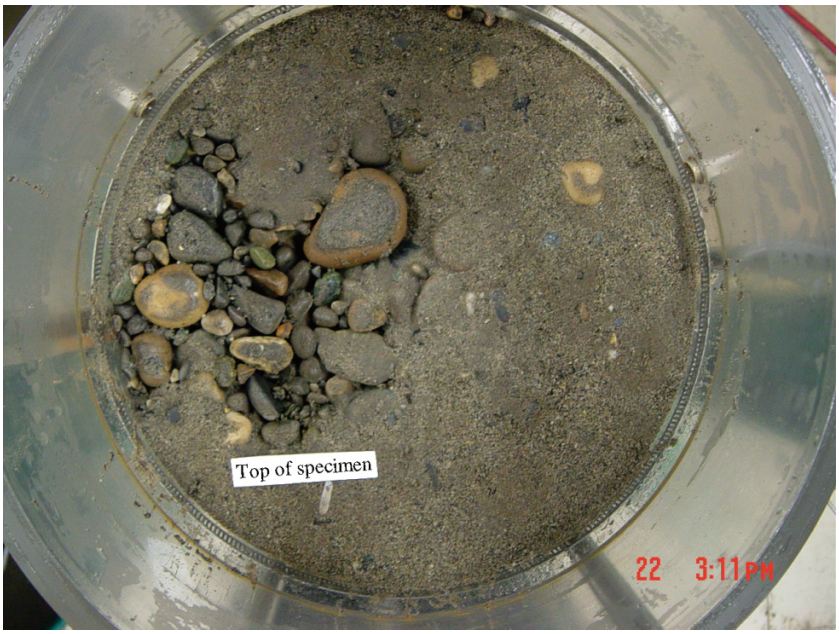

subjected to upward flow. Seepage flow was initiated at $i_{av} = 1$ and increased sequentially to failure at $i_{av} = 32$ over a cumulative time of nearly 32 h of seepage (Table 1). The variation of unit displacement with increasing i_{av} shows negligible vertical movement to $i_{av} \leq 4$ (Fig. 3). A small displacement at $i_{av} = 5$ was followed by a trend of very small incremental movement to $i_{av} = 31$. Upon increasing the differential head to apply i_{av} greater than 31, a relatively large axial displacement occurred that is attributed to the onset of significant internal erosion.

The variation of local hydraulic gradient with time during the final stage is shown in Fig. 8, with the negative value of i_{jk} indicating upward flow. A value of $i_{av} = 31.3$ was imposed slowly over a period of nearly 175 s, at which time the onset of instability occurred. Similar values of i_{34} and i_{45} are attributed to homogeneity of the central portion of the specimen; they contrast with the relatively lower value of i_{23} that is attributed to seepage-induced fines loss at the downstream (top) surface of the specimen. The smallest value of i_{67} was a result of particle loss during the process of specimen reconstitution. The onset of instability was characterized by a sudden decrease in i_{34} that is attributed to a local increase in hydraulic conductivity as a consequence of particle migration from that layer. Once again, the companion increase in i_{45} and i_{56} was a consequence of the head-control system for seepage flow.

As reported for test T-0-25-D, minor episodic loss of finer particles was also observed in many stages of the test on T-5-175-U. Given the condition of upward flow, it generally took the form of a "boiling" action above openings of the top loading plate; occasionally it appeared as a similar action within voids of the specimen itself, at the contact with the wall of the permeameter. It was only during the last stage of the test that much of the soil specimen lost a considerable part of its finer fraction. At $t \approx 175$ s (Fig. 8), particle movement was observed in the lower portion of the specimen (near port 3, see inserted diagram of Fig. 3) where it retrogressed quickly in the upstream direction. The action resulted in development of an open network of conduits from the top to the bottom of the specimen (compare Figs. 9*a* and 9*b*). Upon stopping the test at $t \approx 225$ s, forensic examination revealed that washed-out sand and silt had settled on the top loading plate. The specimen itself appeared uniform, but devoid of its finer fraction. Individual voids were evident in its lowermost portion, yielding a series of interconnected "pipes" in much of the cross-sectional area of the specimen.

Gravelly, silty sand (test C-20-50-U)

The C-20 soil was consolidated under a top vertical effective stress of 50 kPa, to an initial length of 340 mm, and then subjected to upward flow. Seepage flow was initiated at $i_{av} = 1.0$ and increased to $i_{av} = 27$ over a cumulative time of nearly 112 h of seepage flow (Table 1). Axial displacement was negligible until the onset of failure (Fig. 3).

The variation of local hydraulic gradient with time during the final stage of the test (Fig. 10) indicates values of i_{jk} that again are spatially variable, yet constant with time, implying stability to an elapsed time $t \approx 90$ s. The onset of significant instability is evident from the sudden decrease in i_{56}. The companion increase of i_{45} was again a consequence of the head-control system seeking to maintain i_{av} constant. In the uppermost zone, i_{34} diminished from a value of 8 to 0 in about 25 s, as axial compression of the specimen caused the top plate to settle below the location of port 3 on the permeameter wall. Prior to the test being stopped, an accumulation of washed-out particles on the top loading plate resulted in a modest gradient developing across this newly formed deposit.

Visual observations confirm an episodic loss of finer fraction particles during test stages to $i_{av} = 26$. Imposing $i_{av} = 27$ triggered a sudden movement of particles within the lower portion of the specimen, and led quickly to an energetic "boiling" action at the top of the specimen that was accom-

Fig. 8. Onset of instability: test T-5-175-U (i_{av} = 31.3).

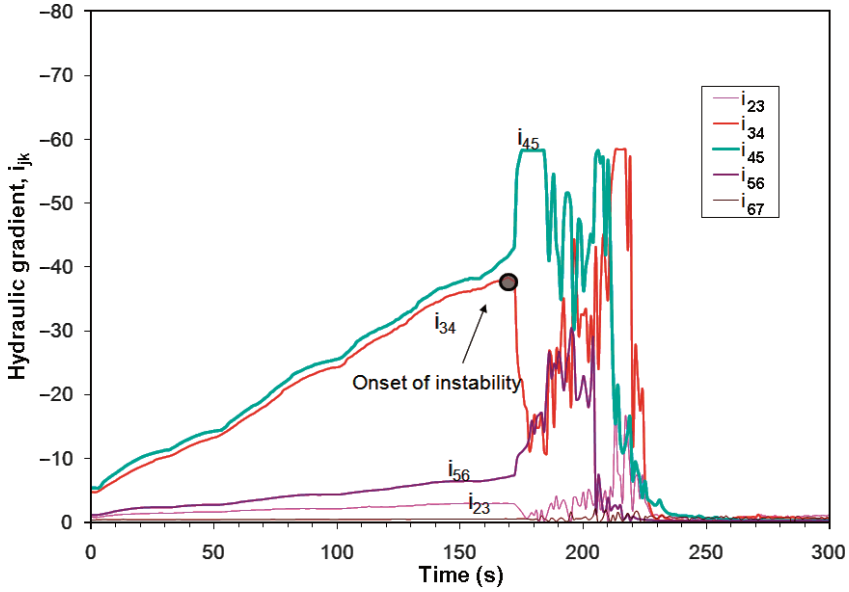

Fig. 9. Test specimen T-5-175-U: (*a*) before failure, i_{av} = 29; (*b*) after failure, i_{av} = 31.3.

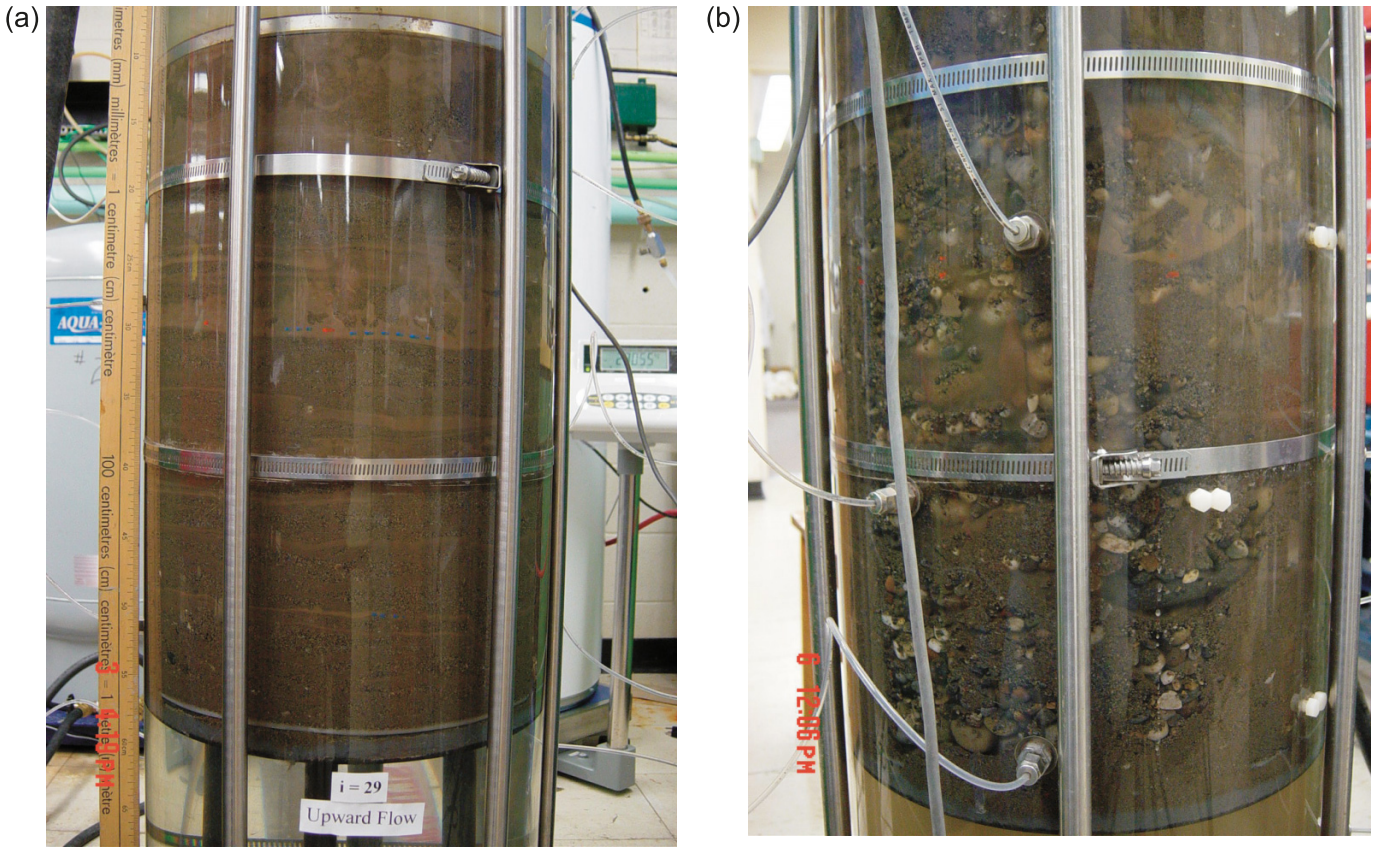

panied by distinct "eruptions" of finer fraction. The onset of instability was characterized by a progressive advance in the direction of seepage flow, commencing near the upstream (lower) boundary. Importantly, no preferential erosion was observed at the walls of the permeameter. Subsequent forensic examination revealed the upper portion of the specimen to have local zones with little or no fines, and the presence of a "pipe" of fines-deficient medium to coarse sand and gravel that began about 40 mm below its top surface. Additional "pipes" were encountered within the mid-to-lower portion of the specimen, which were not evident at the permeameter wall (see Fig. 11).

Gravelly, silty sand (test C-30-80-U)

The C-30 soil was consolidated under a top effective vertical stress of 80 kPa, to an initial length of 335 mm, and

Fig. 10. Onset of instability: test C-20-50-U (i_{av} = 27).

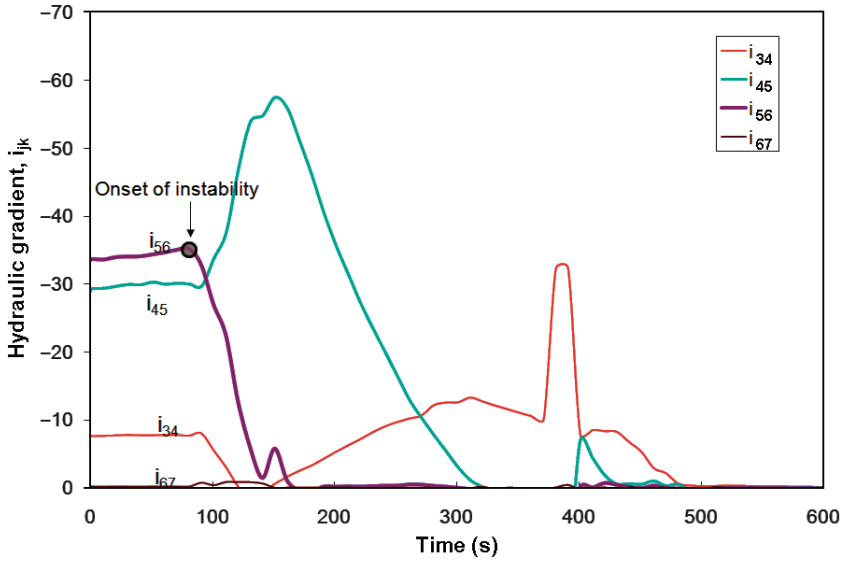

Fig. 11. Test specimen C-20-50-U: (*a*) before failure, i_{av} = 1.0; (*b*) after failure, i_{av} = 27.

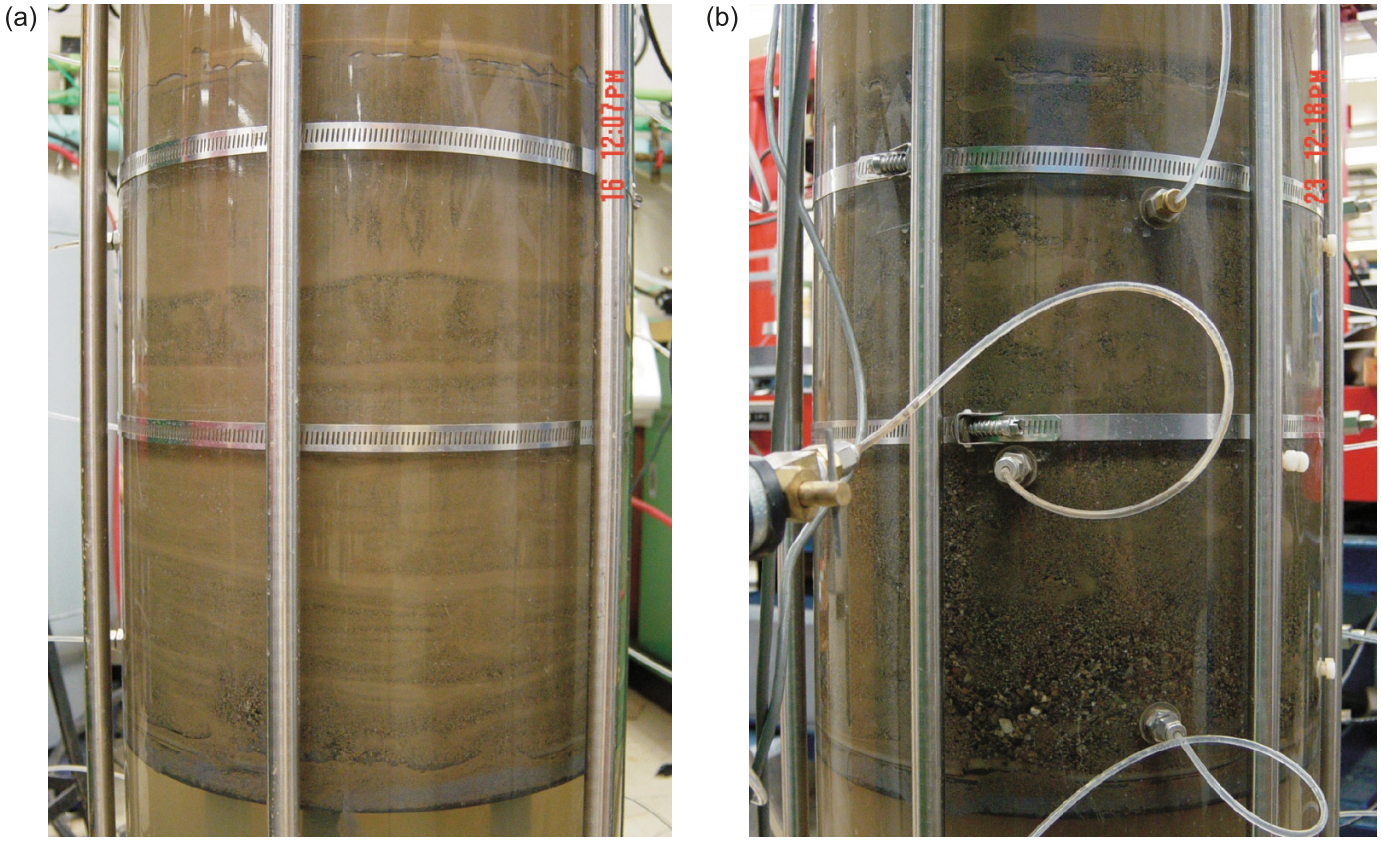

then subjected to upward flow. Seepage flow was initiated at i_{av} = 1 and increased by increments of approximately 1 to a value i_{av} = 29 over a cumulative time of nearly 193 h (Table 1). Negligible axial displacement occurred through to i_{av} = 28, prior to the onset of internal instability (see Fig. 3).

An increase to i_{av} = 29 in the final stage of the test yielded values of i_{jk} that were nearly constant through to an elapsed time $t \approx$ 6500 s (Fig. 12). More specifically, i_{34} exhibited a time-dependent increase and i_{56} a time-dependent decrease, with i_{45} remaining essentially constant. The behavior is attributed to a slow yet steady particle migration within the specimen. Thereafter, i_{45} exhibited a sudden decrease that is believed a consequence of significant localized instability. A companion and very large increase occured in i_{34}. The changes are attributed to soil particles migrating from the lower portion of the specimen and a reaction of the head-control system that attempts to impose a constant

Fig. 12. Onset of instability: test C-30-80-U (i_{av} = 29).

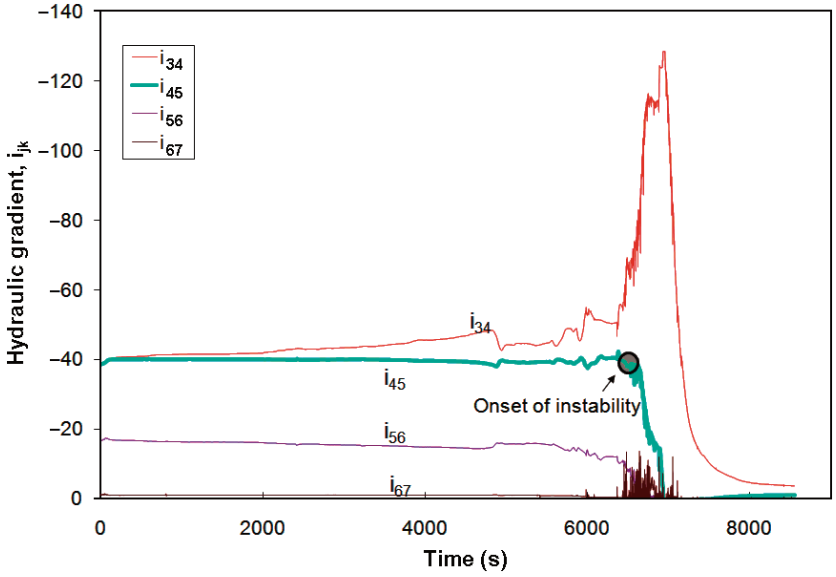

value of i_{av}. As reported for the other tests, the very small value of i_{67} was a result of some particle loss during specimen reconstitution.

Visual observations revealed very little migration of finer fraction materials at the top of the specimen for $1 < i_{av} < 28$, and no indication of impending failure prior to the onset of instability. At i_{av} = 29, a short horizontal flow channel was observed to develop in the middle of the specimen, between port locations 4 and 5 (see inserted diagram of Fig. 3), after an elapsed time t $\approx$ 5000 s. Its development likely explains the change in i_{jk} evident at the same time (see Fig. 12). Subsequently, an outburst of finer fraction particles was observed in the central zone of the top surface of the specimen at $t \approx 6500$ s, which suggests a progressive advance of instability in the direction of seepage flow. At this time, no particle migration was observed at the wall of the permeameter. Thereafter, a zone with little or no finer fraction was observed at the upstream end of the specimen between ports 5 and 7, in which a "boiling" action was evident in loose particles. Small pipes then developed at two locations, a prelude to catastrophic failure in which migration of the finer fraction occurred at many locations and, at $t \approx 7200$ s, a continuous pipe developed through the entire specimen (see Fig. 13). Forensic observations revealed a concentrated and very localized wash-out of finer fraction in the zone of piping activity.

Spatial and temporal progression of instability

Internal instability occurs where grains of the finer fraction migrate through interstices of the matrix formed by the coarser fraction. Accordingly, instability in the test specimen is associated with an increase in void ratio (e) and, given the commensurate loss of finer grains, an increase in the characteristic grain size (D_s). The Kozeny–Carman equation for the intrinsic permeability of a saturated porous medium establishes

$$[1] \qquad K = k\left(\frac{\mu}{\gamma}\right) = \frac{1}{k_o T^2 S_o^2}\left(\frac{e^3}{1+e}\right)$$

Mitchell and Soga (2005) observe the hydraulic conductivity may be written as

$$[2] \qquad k = CD_s^2\left(\frac{\gamma_w}{\mu}\right)\frac{e^3}{1+e}S^3$$

which establishes it to be proportional to $e^3/(1 + e)$ and to D_s, hence a localized increase in e or D_s leads to a corresponding localized increase in conductivity of the soil. As changes in i_{jk} correlate inversely with changes in hydraulic conductivity, the occurrence of instability is defined by a decrease in i_{jk} with time. Thereafter, spatial and temporal variations in i_{jk} may be used to further characterize the instability phenomena observed in testing.

Suffusion

Movement of the finer fraction was most evident visually in tests with downward seepage flow. At times it occurred as a uniform loss across the entire base of the specimen, visible through the wall of the permeameter. Periodically it occurred as a preferential loss from discrete locations on the base, and those locations would vary from stage to stage in any test. The loss was a transient phenomenon, with its onset being coincident with an increment of hydraulic gradient, and the rate of loss diminished thereafter with elapsed time to negligible quantities (see Fig. 5*b*, for test T-0-25-D). Tests with upward seepage flow did not, and likely could not, exhibit such clear visual indications of migration of the finer fraction.

In contrast to the T-0 gradation, the T-5, C-20, and C-30 gradations all have a fines content of silt-sized particles, ranging from 5% to 30%, respectively (Fig. 1). Particle movement in these gradations was less of a transient phenomenon, rather it occurred throughout the duration of a test, and most noticeably in the early and again in the later stages of seepage flow. For example, a time-dependent de-

Fig. 13. Test specimen C-30-80-U: (*a*) before failure, i_{av} = 17; (*b*) after failure, i_{av} = 29.

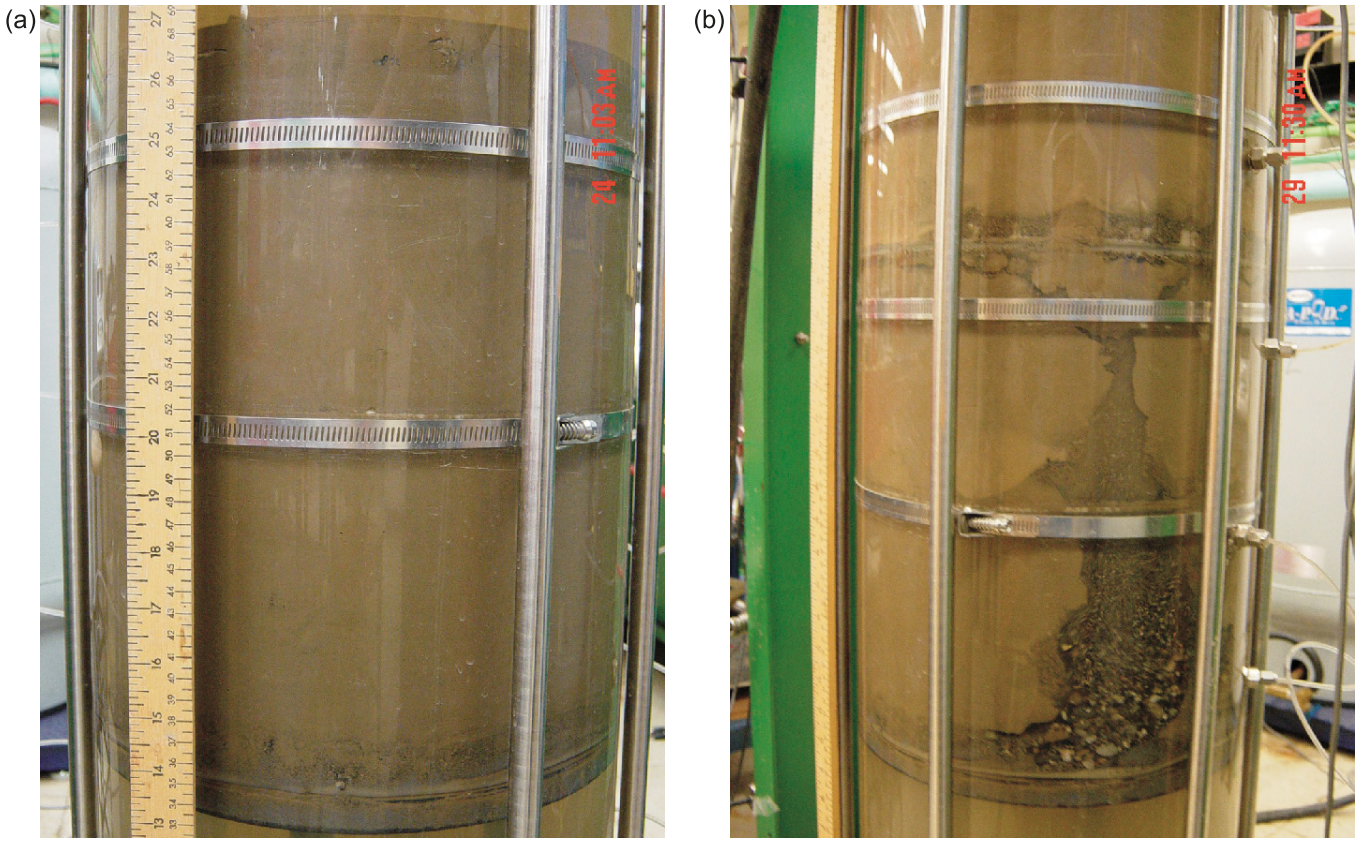

crease in i_{34} and i_{45} over a period of nearly 24 h in test C-30-80-U at i_{av} = 24 (see Fig. 14) is attributed to ongoing loss of fines from the upper portion of the specimen. The loss was not associated with any significant movement of the top plate assembly (see Fig. 3).

The visual observations, and the companion spatial and temporal variations of local hydraulic gradient, reveal a transport of finer particles from the soil with each increment of hydraulic gradient that yields a relatively slow and small change in local permeability, but no change in volume. The response accords well with the phenomenon of suffusion as described by Kovacs (1981). It was evident, to a varying extent, in all four gradations. The suffusion phenomenon appears time-dependent, and is different in character to the sudden onset of instability that occurred in the final stage of testing.

Suffosion

Particle movement was found distinctly preferential in the final stage of a test. It led to development of significant voids in the specimen, which could be inspected through the wall of the permeameter. Periodically, a void was observed either to collapse or to infill with smaller grains. Accordingly, the spatial location of preferential seepage flow varied transiently within the specimen. For the case of upward seepage, the motion of finer grains within a void indicated they were unconstrained by the primary fabric of the soil matrix. The motion was accompanied by a downward displacement of the top plate assembly (see Fig. 3) that sometimes generated an audible grinding sound, likely resulting from a rearrangement of particles forming the soil matrix. The phenomenon was also accompanied by a change in load, and therefore effective stress, on the base of the specimen (for example, see Fig. 15 for test T-0-25-D and compare with Fig. 4); recall that a constant load was imposed on the top of the specimen by the control system.

Inspection of the last stage of seepage flow reveals subtle variations in the spatial and temporal variation of i_{jk} (Moffat 2005). In the coarse-grained soil with no fines content (T-0), the onset of instability was often found to occur after 100 to 500 s of seepage flow at the new increment of hydraulic gradient, and in many, but not all, cases "pipes" were observed shortly thereafter. The coarse-grained soil with some fines (T-5) yielded a similar behavior. In the soils with significant fines content (C-20 and C-30), the onset of instability was often found to occur after 100 to 5000 s of elapsed seepage flow. In contrast to the coarser-grained soils, the resulting zone of instability was found to be more localized.

Visual observations, and the companion spatial and temporal variations of local hydraulic gradient, reveal a particle loss that yields a relatively large and rapid change in local permeability and a companion change in specimen volume. In contrast to the preceding phenomenon of suffusion, this sudden onset of more significant change is deemed characteristic of suffosion.

Piping

In general, the last stage of testing was characterized by (*i*) localized instability followed by re-establishment of a stable equilibrium (e.g., Fig. 4), (*ii*) localized instability fol-

Fig. 14. Variation of hydraulic gradient with time: test C-30-80-U (i_{av} = 24).

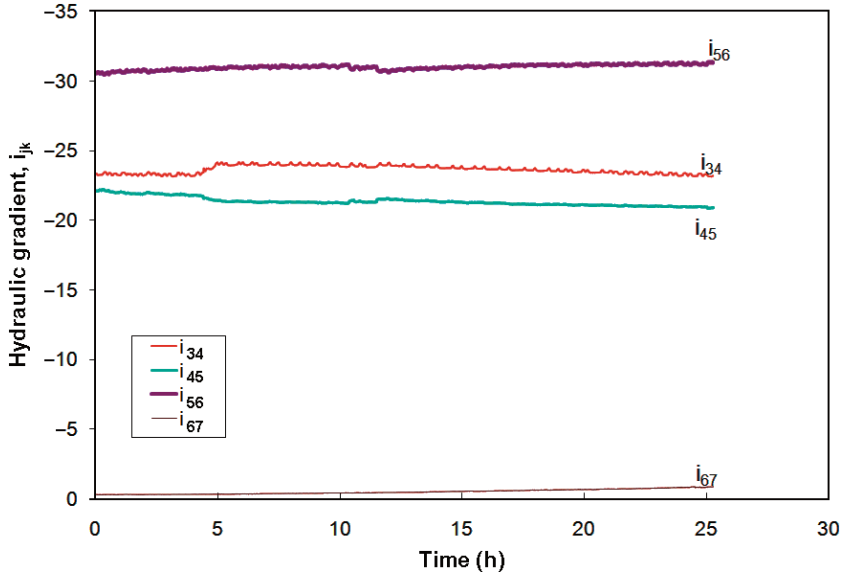

Fig. 15. Variation of boundary stress with time: T-0-25-D (i_{av} = 11).

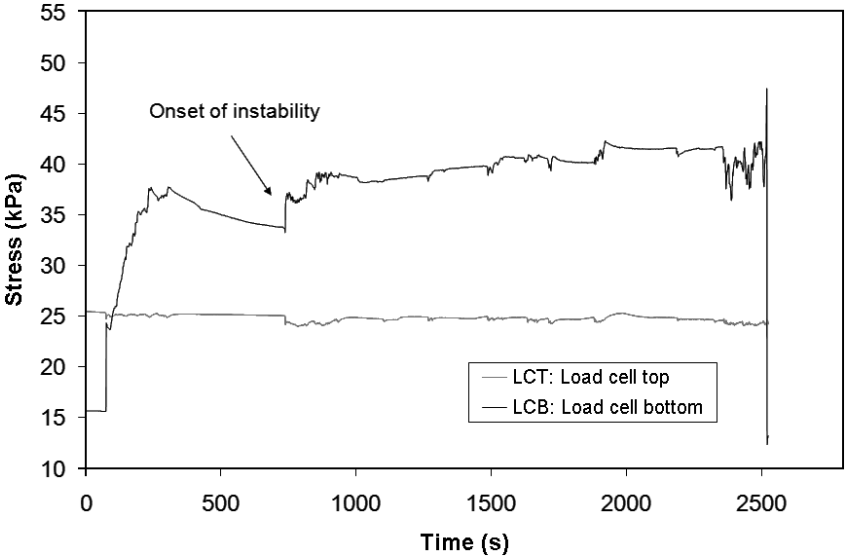

lowed by a period of unstable equilibrium with the specimen (e.g., Fig. 8) or (*iii*) localized instability that triggered an immediate failure throughout the specimen (Figs. 10 and 12). Piping was observed in some, but not all, tests. It occurred primarily in tests that were subjected to continued seepage flow beyond the onset of suffosion. Flow was observed to concentrate in a preferential pathway. The pathway was typically vertical, but would also include a short portion that was diagonal and occasionally horizontal. The spatial extent of the pathway appeared to diminish in size with increasing fines content of the specimen, leading to the development of a more well-defined "pipe" in the C-20 and C-30 soils (compare for example the T-5 gradation in Fig. 9 with the C-30 gradation in Fig. 13). The more localized expression of piping activity in the silty soils did not appear to develop through the entrainment of the finer fraction of the soil in the same extensive manner observed in the T-0 and T-5 soils. Indeed, forensic grain size analysis of exhumed horizontal strata in the C-20 and C-30 soils revealed no change from the original gradation, which suggests the relatively small extent of the piping zone in the silty soil was insufficient to provide for easy detection by this method.

Susceptibility to seepage-induced instability

The experimental results clearly demonstrate that all four soils exhibit internal instability as a result of seepage flow. The T-0 and T-5 gradations are potentially unstable (see Fig. 2*a*) according to the empirical criterion of Kenney and Lau (1986), a finding that imparts further confidence to its use in practice for coarse-grained soils. The C-20 and C-30 soils, which are considerably finer than those tested by Kenney and Lau (1985), are also deemed potentially unstable according to the same empirical criterion (Fig. 2*a*); the experimental results imply that use of the criterion may also

be appropriate for coarse-grained soils with a fraction of silt-sized particles. Likewise, all four gradations are deemed potentially unstable (see Fig. 2*b*) according to the empirical criterion of Kezdi (1979), which was originally conceived for coarse-grained soils. Accordingly, the findings impart further confidence to use of both criteria, and therefore to the unified approach for evaluating susceptibility of a gradation to internal instability proposed by Li and Fannin (2008). The onset of instability appears governed by a critical value of hydraulic gradient, for which a governing "hydromechanical" relation is proposed in stress–gradient space (Moffat and Fannin 2011).

Conclusions

The general nature of internal instability in four widely graded cohesionless soils has been examined using laboratory permeameter test results. The rigid wall of the permeameter did not yield a preferential seepage path. Visual observations, together with measurements of spatial and temporal change in water head distribution along the length of the test specimen, enable a physical characterization of instability. The following conclusions are drawn regarding the instability phenomena of suffusion, suffusion, and piping:

(1) Empirical methods of Kezdi (1979), and of Kenney and Lau (1985, 1986), to evaluate the susceptibility of a gradation curve to internal instability suggest the four soils examined in testing are potentially unstable, and laboratory results establish that to be true. Although the two empirical methods were developed for coarse-grained soils, the experimental observations suggest they may also apply to sands and gravels with a fraction of silt.

(2) Suffusion was observed and took the form of episodic migration of the finer fraction. It was triggered by imposing an increment of i_{av}, and detected visually in all four soils tested. It appears to be a time-dependent phenomenon, as evident from changes in local hydraulic gradient in the soils with significant silt content. Particle migration yields a relatively small and slow change in local hydraulic conductivity, but no change in specimen volume.

(3) Suffosion took the form of loss of finer fraction particles, yielding a relatively large and fast change in local hydraulic conductivity and a consequent change in specimen volume. Visual observations indicate suffosion can be either retrogressive or progressive. It was also triggered by imposing an increment of i_{av}, and detected from visual observations together with changes in local hydraulic gradient, axial displacement, axial load, and an accompanying noise attributed to rearrangement of particles.

(4) The spatial and temporal progression of instability may be characterized by (*i*) localized erosion followed by re-establishment of a stable equilibrium, (*ii*) localized erosion followed by a period of unstable equilibrium within the specimen or (*iii*) localized erosion that triggers a particle migration within the whole specimen. The onset of instability, and its subsequent progression, is believed to be governed by a critical combination of hydraulic gradient and effective stress (Moffat and Fannin 2011, companion paper).

Acknowledgment

The experimental work was conducted in collaboration with British Columbia Hydroelectric Power Authority, which provided financial support and supplied soils used in the testing program.

References

Bates, R.L., and Jackson, J.A. (*Editors*). 1987. Glossary of geology. 3rd ed. American Geological Institute, Washington, D.C.

Bendahmane, F., Marot, D., and Alexis, A. 2008. Experimental parametric study of suffusion and backward erosion. Journal of Geotechnical and Geoenvironmental Engineering, **134**(1): 57–67. doi:10.1061/(ASCE)1090-0241(2008)134:1(57).

CDA. 2007. Geotechnical considerations for dam safety. Canadian Dam Association (CDA), Moose Jaw, Sask. Technical bulletin.

Chapuis, R.P. 1992. Similarity of internal stability criteria for granular soils. Canadian Geotechnical Journal, **29**(4): 711–713. doi:10.1139/t92-078.

de Mello, Y.F.B. 1975. Some lessons from unsuspected, real and fictitious problems in earth dam engineering in Brazil. *In* Proceedings of the 6th Regional Conference for Africa on Soil Mechanics and Foundation Engineering, Durban, South Africa, 8–12 September 1975. National Building Research Institute, CSIR, Pretoria, South Africa. pp. 285–304.

Fannin, R.J., and Moffat, R. 2006. Observations on internal stability of cohesionless soils. Géotechnique, **56**(7): 497–500. doi:10.1680/geot.2006.56.7.497.

Fell, R., MacGregor, P., Stapleton, D., and Bell, G. 2005. Geotechnical engineering of dams. Taylor & Francis Group, plc, London.

Garner, S.J., and Fannin, R.J. 2010. Understanding internal erosion: a decade of research following a sinkhole event. The International Journal on Hydropower and Dams, **17**(3): 93–98.

Garner, S.J., and Sobkowicz, J.C. 2002. Internal instability in gap-graded cores and filters. *In* Proceedings of the Canadian Dam Association Annual Conference, 6–10 October 2002, Victoria, B.C. Available from www.cda.ca/proceedings%20datafiles/2002/2002-07-01.pdf [accessed 11 February 2011].

ICOLD 1978. Technical dictionary on dams. 3rd ed. International Commission on Large Dams, Paris.

ICOLD. 1986. Geotextiles as filters and transitions in fill dams. International Commission on Large Dams (ICOLD), Paris. Bulletin 55.

Kenney, T.C., and Lau, D. 1985. Internal stability of granular filters. Canadian Geotechnical Journal, **22**(2): 215–225. doi:10.1139/t85-029.

Kenney, T.C., and Lau, D. 1986. Internal stability of granular filters: Reply. Canadian Geotechnical Journal, **23**(3): 420–423. doi:10.1139/t86-068.

Kezdi, A. 1979. Soil physics. Elsevier, Amsterdam.

Kovacs, G. 1981. Seepage hydraulics. Elsevier, Amsterdam.

Li, M., and Fannin, R.J. 2008. Comparison of two criteria for internal stability of granular soil. Canadian Geotechnical Journal, **45**(9): 1303–1309. doi:10.1139/T08-046.

Li, M., Fannin, R.J., and Garner, S.J. 2009. Application of a new criterion for assessing the susceptibility to internal erosion. *In* Proceedings of the Canadian Dam Association Annual Conference, Whistler, B.C., 3–8 October 2009. Available from www.cda.ca/proceedings%20datafiles/2009/2009-9b-03.pdf [accessed 11 February 2011].

Milligan, V. 1986. Internal stability of granular filters: Discussion. Canadian Geotechnical Journal, **23**(3): 414–418. doi:10.1139/t86-066.

Mitchell, J.K., and Soga, K. 2005. Fundamentals of soil behavior. 3rd ed. John Wiley & Sons, Inc., Hoboken, N.J.

Moffat, R. 2005. Experiments on the internal stability of widely-graded cohesionless soils. Ph.D. thesis, The University of British Columbia, Vancouver, B.C.

Moffat, R., and Fannin, R.J. 2006. A large permeameter for study of internal stability in cohesionless soils. Geotechnical Testing Journal, **29**(4): 273–279. doi:10.1520/GTJ100021.

Moffat, R., and Fannin, R.J. 2011. A hydromechanical relation governing internal stability of cohesionless soil. Canadian Geotechnical Journal, **48**(3): 413–424. [Companion paper.] doi:10.1139/T10-070.

Morgan, G.C., and Harris, M.C. 1967. Portage Mountain dam: II. Materials. Canadian Geotechnical Journal, **4**(2): 142–166. doi:10.1139/t67-031.

OED online. 2010. Oxford English dictionary. 2nd ed. 1989 [online version November 2010]. Available from www.oed.com/view/entry/193575 [accessed 31 January 2011].

Raut, A.K. 2006. Mathematical modelling of granular filters and constriction-based filter design criteria. Ph.D. thesis, University of Wollongong, Wollongong, Australia.

Reddi, L.N., Lee, I.-M., and Bonala, M.V.S. 2000. Comparison of internal and surface erosion using flow pump tests on a sand-kaolinite mixture. Geotechnical Testing Journal, **23**(1): 116–122. doi:10.1520/GTJ11129J.

Richards, K.S., and Reddy, K.R. 2007. Critical appraisal of piping phenomena in earth dams. Bulletin of Engineering Geology and the Environment, **66**(4): 381–402. doi:10.1007/s10064-007-0095-0.

Ripley, C.P. 1967. Portage Mountain dam: I. An outline of the project. Canadian Geotechnical Journal, **4**(2): 125–138. doi:10.1139/t67-027.

Sherard, J.L. 1979. Sinkholes in dams of coarse, broadly graded soils. *In* Transactions of the 13th International Congress on Large Dams, New Delhi, India, 29 October – 2 November 1979. International Commission on Large Dams, Paris. Vol. 2, pp. 25–34.

Skempton, A.W., and Brogan, J.M. 1994. Experiments on piping in sandy gravels. Géotechnique, **44**(3): 449–460. doi:10.1680/geot.1994.44.3.449.

Stewart, R.A., and Watts, B.D. 2000. The WAC Bennett Dam sinkhole incident. *In* Proceedings of the 53rd Canadian Geotechnical Conference, Montréal, Que., 15–18 October 2000. BiTech Publishers Ltd., Richmond, B.C. Vol. 1, pp. 39–46.

Wan, C.F., and Fell, R. 2008. Assessing the potential of internal instability and suffusion in embankment dams and their foundations. Journal of Geotechnical and Geoenvironmental Engineering, **134**(3): 401–407. doi:10.1061/(ASCE)1090-0241(2008)134:3(401).

List of symbols

C	composite shape factor
D	grain size
D_s	characteristic grain size
D'_{15}	grain size corresponding to 15% finer (used for the coarser fraction or filter layer)
d'_{85}	grain size corresponding to 85% finer (used for the finer fraction or base layer)
e	void ratio
F	mass fraction smaller than D
H	mass fraction measured between particles sizes D and $4D$ (Kenney and Lau 1985)
i_{av}	average hydraulic gradient
i_{jk}	hydraulic gradient between ports j and k
K	intrinsic permeability
k	hydraulic conductivity
k_o	pore shape factor
L_c	soil specimen length
S	degree of saturation
S_o	wetted surface area per unit volume
T	tortuosity factor
t	time
δ	axial displacement
γ	unit weight of permeant (water)
μ	viscosity of permeant (water)